The Journal of Engineering

The 14th IET International Conference on AC and DC Power Transmission (ACDC 2018)

IET Journals
The Institution of Engineering and Technology

Impact analysis of traction loads on power grid based on probabilistic three-phases load flow

eISSN 2051-3305
Received on 23rd August 2018
Accepted on 19th September 2018
E-First on 19th December 2018
doi: 10.1049/joe.2018.8532
www.ietdl.org

Yulong Che[1,2,3], Xiaoru Wang[1] ✉, Xiaoqin Lv[1], Yi Hu[1], Longyuan Li[1], Haoyue Chen[1]

[1]*School of Electrical Engineering, Southwest Jiaotong University, Chengdu, People's Republic of China*

[2]*School of Automation and Electrical Engineering, Lanzhou Jiaotong University, Lanzhou, People's Republic of China*

[3]*Rail Transit Electrical Automation Engineering Laboratory of Gansu Province, Lanzhou Jiaotong University, Chengdu, People's Republic of China*

✉ *E-mail: xrwang@home.swjtu.edu.cn*

Abstract: Electrified railway traction power supply system is directly powered by 110 kV or 220 kV (some 330 kV) high-voltage power grid. The uncertainty, non-linearity, and asymmetry of traction loads like the electric locomotives and electric multiple units (EMUs) exert the negative sequence and harmonics impact on the high-voltage transmission network. In order to evaluate the impact of the uncertainty and asymmetry of traction loads on the high-voltage transmission grid, a probabilistic three-phase power flow model of transmission network considering the probability model of traction loads is proposed. First, the power probability model of traction loads is established according to the running characteristics of traction loads. Second, the Monte Carlo simulation method is applied for the probabilistic three-phase power flow model calculation considering the traction loads. Finally, the simulation calculation is carried out on the balanced IEEE-14 bus three-phase test system. The results show that the asymmetric traction loads cause the unbalance of the grid nearby to deteriorate. The further away from the traction substation, the smaller impact of the traction loads.

1 Introduction

With the rapid development of AC electrified railway, it has been brought freight transport convenience, traveling convenience, and shortening the distance between cities. Meanwhile, the high-speed and high-power electric locomotives or electric multiple unit (EMU) need more power. Due to the asymmetry, volatility, and non-linearity of the traction power supply system (TPSS), these cause more serious problems for the power grid, such as the unbalances and harmonics [1]. The traction loads of TPSS is uncertain, owing to the uncertainties about trains operation affected by the factors such as weather, routes, speed limits of trains etc.

The most commonly used power supply mode of electric railway is auto transformer (AT) power supply. All parallel AT-fed double-line traction network is a total of 14 conductors with a multi-conductors complex network [2]. Literatures [3–6] studied the power flow calculation of AT TPSS. However, the traction loads of TPSS is not considered in the power grid for power flow calculation, therefore the influence of the asymmetry and randomness of the traction power supply system on the power grid cannot be analysed. The probabilistic power flow of TPSS is a study considering the uncertainties or possible changes in the weather, train speeds, train schedules etc. [7–9]. However, the influence of traction loads characteristics on the power system was not been studied, such as the asymmetry and randomness of TPSS.

Taking into account the asymmetry and uncertainty of the TPSS makes sense to analyse the influence of TPSS included into the power grid. The probabilistic three-phase power flow provides ideas for this issue [10, 11]. Based on the uncertainties with the running process of electric locomotive, the probability model of traction loads is established by the operating power of an electric locomotive and the number of running trains in the traction substation (TS). The three-phase power flow is used to calculate the negative sequence propagation caused by the asymmetric TPSS. The Monte–Carlo simulation method is applied for the probabilistic three-phase power flow computation in the modified balanced IEEE-14 bus three-phase test system considering the traction loads of TPSS. Probability Density Function (PDF) of voltage imbalance, current unbalances of transmission lines, power of transmission lines and network loss are calculated before and after the TPSS is connected to the grid.

2 TPSS and its probability model

2.1 TPSS and ports transformation relationship

TPSS consists of TSs, feeders, traction networks, several autotransformers (ATs) posts, sectioning posts (SPs), and some running trains. The system diagram of TPSS is as shown in Fig. 1. The traction transformer is the most critical equipment in TS, which is a hub linking between the three-phase AC system and the two-phase TPSS. The mainstream modes of TPSS currently are the direct power supply mode with a return stream and the AT power supply mode.

The three-phase 110 kV or 220 kV line voltage is stepped down to the two-phase 27.5 kV or 55 kV by the traction transformer in TS. The electric locomotive is supplied by a single-phase 27.5 kV/55 kV AC feeding circuits with electric power via three-phase to two-phase traction transformers, feeders, and traction networks. When the ground is taken as a common reference point, the primary three-phase system of the traction transformer and the reference point form a three-ports. The secondary two-phase system of the traction transformer constitutes a two-ports. For the sake of research on the unbalance of electrified railway and the distribution of harmonics in power system, a three-phase equivalent model of TPSS needs to be established through the two-phase to three-phase transformation of system.

The three-ports of the primary side of traction transformers are expressed as A, B, C. The two-ports of second side of traction transformers are expressed as α, β. The voltage vectors and the current vectors of three-phases are expressed as $\left[\dot{U}_A, \dot{U}_B, \dot{U}_C\right]^{\mathrm{T}}$ and $\left[\dot{I}_A, \dot{I}_B, \dot{I}_C\right]^{\mathrm{T}}$, respectively. The voltage vectors and the current vectors of two-phases are expressed as $\left[\dot{U}_\alpha, \dot{U}_\beta\right]^{\mathrm{T}}$ and $\left[\dot{I}_\alpha, \dot{I}_\beta\right]^{\mathrm{T}}$, respectively.

Without considering the zero sequence in the ports of traction transformation, the transformation of terminal voltages is assumed by

This is an open access article published by the IET under the Creative Commons Attribution License (http://creativecommons.org/licenses/by/3.0/)

$$U_{ABC} = N_2 U_{\alpha\beta} \tag{1}$$

and the inverses transformation is expressed by

$$U_{\alpha\beta} = N_2^{-1} U_{ABC} \tag{2}$$

where N_2, N_2^{-1} are the transformational matrix and inverse transformation matrix of terminal voltages, respectively.

The transformation of terminal currents is assumed by

$$I_{ABC} = M_2 I_{\alpha\beta} \tag{3}$$

and the inverses transformation is expressed by

$$I_{\alpha\beta} = M_2^{-1} I_{ABC} \tag{4}$$

where M_2, M_2^{-1} are the transformational matrix and inverse transformation matrix of terminal currents, respectively.

The common wiring of traction transformer in TPSS is YNd11 wiring, V/v (or V/x) wiring, and Scott wiring. Taking the V/v wiring as an example, the transformational matrices N_2, N_2^{-1}, M_2, and M_2^{-1} are expressed as follows [12].

$$N_2 = \frac{1}{3K}\begin{bmatrix} 2 & 1 \\ -1 & 1 \\ -1 & 2 \end{bmatrix}, \quad N_2^{-1} = K\begin{bmatrix} 1 & -1 & 0 \\ 0 & 1 & -1 \end{bmatrix}$$

$$M_2 = K\begin{bmatrix} 1 & 0 \\ -1 & 1 \\ 0 & -1 \end{bmatrix}, \quad M_2^{-1} = \frac{1}{3K}\begin{bmatrix} 2 & -1 & -1 \\ 1 & 1 & -2 \end{bmatrix}$$

where K is winding ratio between the secondary side and primary side of traction transformer. For example, the primary side is the 220 kV system, then $K = 27.5/220 = 1/8$.

2.2 Three-phase equivalent model of TPSS

The two-phase TPSS model can be converted into an equivalent three-phase system with two parts. The one is traction transformer, the other one is traction loads and parallel compensation equipment. The traction transformer leakage reactance and traction secondary system must be transformed separately, so that the system transformation reflects the actual physical process. Then, these two parts are linked together by the electromagnetic coupling relationship

2.2.1 System transformation of traction transformer: The circuit model for the two-phase system on the traction side can be described in Fig. 2. $Z_{T\alpha}$ and $Z_{T\beta}$ are the equivalent leakage reactance of port α and β winding. $Z_{T\alpha\beta}$ is the mutual leakage reactance between port α and β winding. $Z_{F\alpha}$ and $Z_{F\beta}$ are the impedance of the filter device or parallel compensation device in port α and β. $\dot{I}_{H\alpha}$ and $\dot{I}_{H\beta}$ are the traction loads in port α and β, respectively, as a current source.

The node voltage equations of traction transformer can be obtained from Fig. 2.

$$\begin{bmatrix} \dot{E}_\alpha \\ \dot{E}_\beta \end{bmatrix} = \begin{bmatrix} \dot{U}_\alpha \\ \dot{U}_\beta \end{bmatrix} + \begin{bmatrix} Z_{T\alpha} & Z_{T\alpha\beta} \\ Z_{T\beta\alpha} & Z_{T\beta} \end{bmatrix} \begin{bmatrix} \dot{I}_\alpha \\ \dot{I}_\beta \end{bmatrix} \tag{5}$$

or abbreviated as

$$\boldsymbol{E}_{\alpha\beta} = \boldsymbol{U}_{\alpha\beta} + \boldsymbol{Z}_{T\alpha\beta}\boldsymbol{I}_{\alpha\beta} \tag{6}$$

The leakage reactance array $\boldsymbol{Z}_{T\alpha\beta}$ can be got according to the different wiring of traction transformer. Then with the voltage, current conversion matrix, and its inverse matrix, the traction transformer equation described in (5) or (6) can be transformed into an equivalent three-phase equation, attached the corresponding

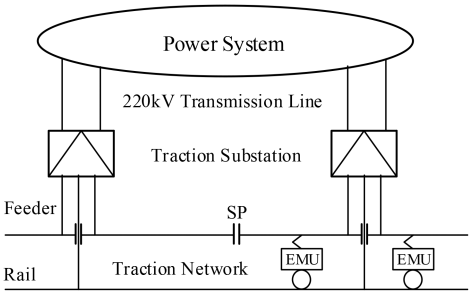


Fig. 1 *Diagram of TPSS*

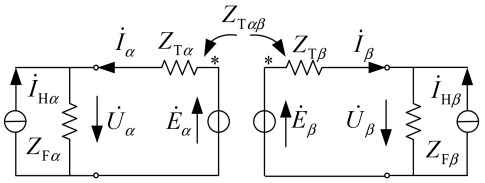


Fig. 2 *Circuit model of TPSS on the traction side*

other transformation matrix. Then the three-phase equivalent model of traction transformer can be achieved.

Multiply (6) with N_2 from the left, and substitute (1) and (4) into (6). The primary-side three-phase voltage equation of traction transformer is

$$\begin{aligned} \boldsymbol{E}_{ABC} &= N_2\boldsymbol{E}_{\alpha\beta} \\ &= N_2^{-1}\boldsymbol{U}_{\alpha\beta} + N_2\boldsymbol{Z}_{T\alpha\beta}M_2^{-1}\boldsymbol{I}_{ABC} \end{aligned} \tag{7}$$

also abbreviated as

$$\boldsymbol{E}_{ABC} = \boldsymbol{U}_{ABC} + \boldsymbol{Z}_{ABC}^{T}\boldsymbol{I}_{ABC} \tag{8}$$

where $\boldsymbol{Z}_{ABC}^{T} = N_2\boldsymbol{Z}_{T\alpha\beta}M_2^{-1}$ is called the three-phase equivalent leakage reactance matrix of traction transformer.

For the V/v wiring traction transformer, let $Z_{T\alpha} = Z_{T\beta} = Z_T$, then the $\boldsymbol{Z}_{ABC}^{T}$ of traction transformer of V/v wiring traction transformer is

$$\boldsymbol{Z}_{ABC}^{T} = \frac{Z_T}{9K^2}\begin{bmatrix} 5 & -1 & -4 \\ -1 & 2 & -1 \\ -4 & -1 & 5 \end{bmatrix}$$

2.2.2 System transformation of traction loads and parallel compensation equipment: The loop voltage equations of traction system containing the filter branch and traction loads can be obtained from Fig. 2.

$$\begin{bmatrix} \dot{I}_\alpha \\ \dot{I}_\beta \end{bmatrix} = \begin{bmatrix} \dot{I}_{H\alpha} \\ \dot{I}_{H\beta} \end{bmatrix} + \begin{bmatrix} Z_{F\alpha} & \\ & Z_{F\beta} \end{bmatrix}^{-1} \begin{bmatrix} \dot{U}_\alpha \\ \dot{U}_\beta \end{bmatrix} \tag{9}$$

abbreviated as

$$\boldsymbol{I}_{\alpha\beta} = \boldsymbol{I}_{\alpha\beta}^{H} + \boldsymbol{Z}_{F\alpha\beta}^{-1}\boldsymbol{U}_{\alpha\beta} \tag{10}$$

When $\boldsymbol{Z}_{F\alpha\beta}$ is non-singular, (10) can be transformed into a three-phase system using the voltage and current transform matrix. That is

$$\boldsymbol{I}_{ABC} = \boldsymbol{I}_{ABC}^{H} + \boldsymbol{Y}_{FABC}\boldsymbol{U}_{ABC} \tag{11}$$

where $\boldsymbol{Y}_{FABC} = M_2(\boldsymbol{Z}_{F\alpha\beta})^{-1}N_2^{-1}$ is called an equivalent three-phase admittance array of parallel compensation network; $\boldsymbol{I}_{ABC}^{H} = M_2\boldsymbol{I}_{F\alpha\beta}$ is called an equivalent three-phase admittance array of current source.

This is an open access article published by the IET under the Creative Commons Attribution License (http://creativecommons.org/licenses/by/3.0/)

Uniting (8) and (11), a three-phase equivalent model of TPSS associated with the gird can be obtained, as shown in Fig. 3.

where $\boldsymbol{E}_{ABC}^{\mathrm{S}}$ is the power system three-phase voltage array; $\boldsymbol{Z}_{ABC}^{\mathrm{S}}$ is the power system three-phase impedance array.

An unbalanced three-phase power system model considering the TSSS model can be formed by substituting the three-phase equivalent model of TPSS into a three-phase grid.

2.3 Probabilistic model of traction loads

The decisive factor affecting the traction load in TS is the number of electric locomotives and their actual operating power in the power supply interval. As the train starts with reference to the scheduled operation diagram, the number of electric locomotives in the power supply interval has a stable expected value and is subject to the normal distribution in the statistical law due to random factors. For a single electric locomotive and EMU, the main factors affecting its active power include the train parameters and its operating status, line data (including speed limits, ramps and curves) and natural environmental conditions. Although the trains are running with reference to the speed limit, but the actual operating speed must exist some error compared with the speed limit. At the same time, the train loads, line conditions, weather conditions, driving operations, and so on are constantly changing, so the active power will fluctuate randomly around a desired value. According to the law of large numbers and the central limit theorem, the active power of a single electric locomotive passing a single speed limit interval should be subject to the normal distribution in a large sample space [13]. Expressed as,

$$f(x)=\frac{1}{\sqrt{2\pi}\sigma}\exp\left[-\left(\frac{x-\mu}{\sqrt{2}\sigma}\right)^2\right] \tag{12}$$

where f is PDF; x is the random variables of active power or numbers of the electric locomotive; μ is mean values; σ is standard deviations.

Supposing the random variables $A\sim N_P(\mu_P,\sigma_P^2)$ and $B\sim \mathrm{int}\left[N_N(\mu_N,\sigma_N^2)\right]$ represent the active power of a single train and the number of trains in the power supply section, respectively, the total active power can be jointly represented by the random variables A and B. Let the real number c means no-load loss. The simulation of traction loads mainly focuses on the distribution of active power in high values. Let the random variable W denotes the active power of the traction substation [14].

$$W=\sum_{i=1}^{\mathrm{int}(B)}A+c \tag{13}$$

where int is a rounding function that follows the rounding guidelines.

3 Deterministic three-phase load flow

Since the traction loads of the electrified railway are asymmetric loads, it is more difficult to deal with the asymmetric load using the sequence component method. The phase component method is more intuitive, and it is more convenient to handle bus power. Therefore, the phase component method is used to model the three-phase load flow here.

3.1 Imbalance equation of three-phase grid network

The node admittance matrix of three-phase network can be formed once the parameters of the elements (e.g. synchronous machines, transmission lines, transformers, electricity loads and traction loads) in the grid are known. Then, the imbalance equation of active power and reactive power for each phase of each node are as follows.

$$\begin{cases}\Delta P_i^f=P_i^f-V_i^f\sum\limits_{j=1}^{N}\sum\limits_{g=1}^{3}V_j^g\left(G_{ij}^{fg}\cos\theta_{ij}^{fg}+B_{ij}^{fg}\sin\theta_{ij}^{fg}\right)\\ \Delta Q_i^f=Q_i^f-V_i^f\sum\limits_{j=1}^{N}\sum\limits_{g=1}^{3}V_j^g\left(G_{ij}^{fg}\sin\theta_{ij}^{fg}-B_{ij}^{fg}\cos\theta_{ij}^{fg}\right)\end{cases} \tag{14}$$

where f and g are used to denote any one of phases A, B, C; ΔP_i^f and ΔQ_i^f are mismatch powers; P_i^f and Q_i^f represent the given active and reactive power values of each phase of the bus bar; V_i^f is the f-phase of bus no. i; θ_{ij}^{fg} represents the voltage phase angle difference between the f-phase of bus no. i and the g-phase of bus no. j.

The solution to the load-flow equation is the set of variables which make the left-hand-side mismatches in (14) equal to zero.

3.2 Correction equation of three-phase power flow

The Newton–Raphson algorithm is used to solve (14). Suppose the number of PQ nodes is n and the number of PV nodes is m. The correction equation of node voltage expressed as a polar coordinate:

$$\begin{bmatrix}\Delta P^f\\ \Delta Q^f\end{bmatrix}=-\begin{bmatrix}H^{fg} & N^{fg}\\ J^{fg} & L^{fg}\end{bmatrix}\begin{bmatrix}\Delta\theta^g\\ \Delta V^g/V\end{bmatrix} \tag{15}$$

$H_{ij}^{fg}=\dfrac{\partial\Delta P_i^f}{\partial\theta_j^g}$ is $3(n-1)\times 3(n-1)$th order square matrix.

$N_{ij}^{fg}=\dfrac{\partial\Delta P_i^f}{\partial V_j^g}\times V_j^g$ is $3(n-1)\times 3m$th order matrix.

$J_{ij}^{fg}=\dfrac{\partial\Delta Q_i^f}{\partial\theta_j^g}$ is $3m\times 3(n-1)$th order matrix.

$L_{ij}^{fg}=\dfrac{\partial\Delta Q_i^f}{\partial V_j^g}\times V_j^g$ is $3m\times 3m$th order square matrix.

Each variable can be corrected after the correction value of each variable is solved, that is,

$$\begin{cases}\theta_i^{f(k+1)}=\theta_i^{f(k)}+\Delta\theta^{(k)}\\ V_i^{f(k+1)}=V_i^{f(k)}+\Delta V^{(k)}\end{cases} \tag{16}$$

Equations (14) and (15) are solved iteratively in the power flow calculation. The correction value is obtained until the maximum value of the active power and the reactive power is less than a certain limit, $\max\left(\Delta P_i^f,\Delta Q_i^f\right)\le\xi$. The iteration calculation is completed to obtain the power flow calculation result.

3.3 Imbalance analysis of three-phase power flow

The three-phase voltages of all nodes and the three-phase currents of all lines in the grid can be obtained when the calculation of three-phase power flow has been completed. The positive sequence, negative sequence, and zero sequence values of all node voltages and line currents can be easily achieved using the symmetrical component method. When choosing phase A as a reference value, the relationship between the three-phase phasors and its symmetrical component is:

$$\begin{bmatrix}\dot{U}_1\\ \dot{U}_2\\ \dot{U}_0\end{bmatrix}=\frac{1}{3}\begin{bmatrix}1 & a & a^2\\ 1 & a^2 & a\\ 1 & 1 & 1\end{bmatrix}\begin{bmatrix}\dot{U}_A\\ \dot{U}_B\\ \dot{U}_C\end{bmatrix} \tag{17}$$

where $a=\mathrm{e}^{\mathrm{j}120}$, $a^2=\mathrm{e}^{\mathrm{j}240}$, and $1+a+a^2=0$.

This is an open access article published by the IET under the Creative Commons Attribution License (http://creativecommons.org/licenses/by/3.0/)

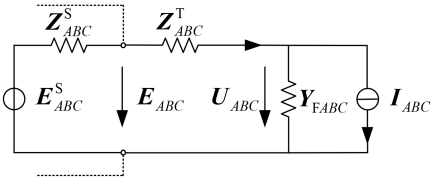


Fig. 3 *Three-phase equivalent model of TPSS*

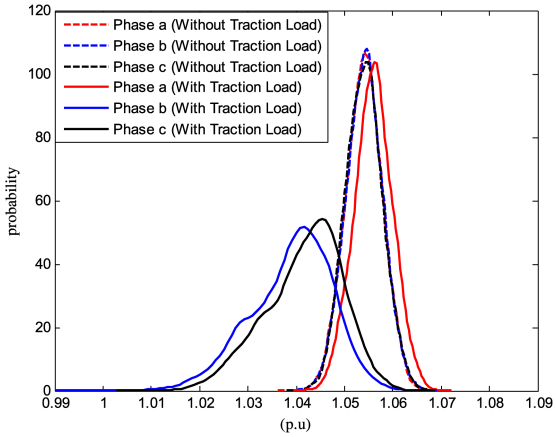


Fig. 4 *PDFs of voltage amplitudes at bus no. 9*

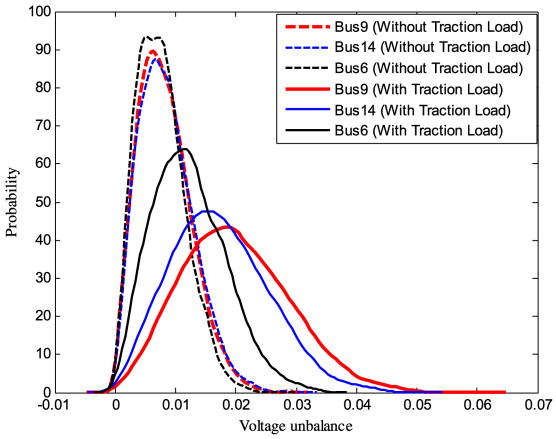


Fig. 5 *PDFs of voltage unbalances at bus no.9, 14 and 6*

4 Monte Carlo procedure

The probabilistic steady-state calculation of an unbalanced three-phase power system can be performed by Monte Carlo simulation method. The basic idea of the Monte Carlo simulation method is to establish a probabilistic analysis model, and then a large number of random variable samples are randomly generated, and finally these sample data are used to calculate the approximate solution of the problem.

The three-phase power flow imbalance equation as shown in (14) can be summarised as:

$$Y = f(X) \tag{18}$$

where X represents the output vector (e.g. amplitude and angle of voltages) of the state variables; Y is the input variable of the system (e.g. active and reactive power of loads); f represents the non-linear three-phases power flow equations.

The active power and reactive power loads of the three-phase power system obey the normal distribution on the basis of the Central Limit Theorem. The random input data can be generated from the probability density function of the three-phase power loads and the probability density distribution of the traction loads in Section 2.3. According to the randomly generated input values, the deterministic non-linear three-phase power flow equations are solved by the Newton–Raphson method introduced in Section 3, and the steady-state conditions of the unbalanced power system can be obtained. Once convergence has been reached, the operating state of the power system is fully known. The values of the output variables of interest, such as the magnitudes and phase angles of the node voltages, the active and reactive power of the transmission lines, and the active power losses are stored. According to the setting accuracy, the above process is repeated with a sufficient number of times to get a good estimate of the statistics parameters of the output variables.

5 Results and discussion

Take a busy freight railway line as an example. The cargo locomotive model for the heavy haul railway is HXD1. The rated power of a 5,000 t single locomotive is 9600 kW. The rated power of a 10,000 t two-locomotive is 19,200 kW. The power factor of HXD1 is 0.97, and the maximum operating speed is 120 km/h. Two V/v wiring transformers are designed for use by the main one and the other one prepared in TSs. The distance of two power supply arms are 25 km. The rated voltage of the traction transformer is $220 \times (1 \pm 2 \times 2.5\%)/27.5$–$27.5$ kV. The rated capacity is $2 \times (31.5 + 31.5)$ MVA. The no-load current percentage is 0.20%. The no-load power loss is 15.74 kW. The short-circuit voltage percentage is 10.5%. The short-circuit power loss 116.78 kW.

In order to analyse the asymmetry and uncertainties of the TPSS, the traction loads of TS is accessed at the bus no. 9. The TS is taken as a new node and it is numbered as bus no.15. The probabilistic model of traction loads is given in Section 2.3. For modelling the randomness in the loads, the active power and reactive power of IEEE-14 bus three-phase system are assumed to be normally distributed. The mean values are the load data given in [15], and the standard deviation equal to 10% of the corresponding average of the load [11]. For performing the impact of asymmetry and randomness of traction loads on the gird from the following four aspects, deterministic three-phase load flow calculations has been carried out 5,000 times.

5.1 Impact of traction loads on grid voltage

The PDFs of phase-voltage amplitudes at bus no. 9 with and without the traction loads obtained by the Monte Carlo procedure are shown in Fig. 4.

From Fig. 4, the PDFs of the three-phase voltage amplitudes of bus no. 9 without the traction loads are coincide substantially, that is, the three-phase voltage is symmetrical. However, the PDFs of the three-phase voltage amplitudes of bus no. 9 with the traction loads are asymmetrical. It can be seen that asymmetric traction loads can cause the voltage amplitudes drop of two phases at bus no. 9, while the other phase voltage amplitude increases slightly.

As only one pair of line voltages are adopted by V/v wiring traction transformers, that is, any one pair line voltages in traction sides are taken in $\dot{U}_{AB}$, $\dot{U}_{BC}$, $\dot{U}_{CA}$ or its reverse $\dot{U}_{BA}$, $\dot{U}_{CB}$, $\dot{U}_{AC}$. Therefore, two-phase voltage amplitudes are dropped and the other phase voltage amplitude is rose slightly in a balanced three-phase system.

5.2 Impact of traction loads on grid imbalance

The PDFs of voltage unbalance at bus nos 9, 14, and 6 are shown in Fig. 5, when the traction loads are connected and not connected at bus no. 9. Bus no. 14 is near bus no. 9 and bus no. 6 is far from bus no. 9.

From the analysis of Fig. 5, it follows that the expected values of the voltage unbalances at bus nos 9, 14, and 6 are 0.83, 0.85, and 0.76%, respectively, when the traction loads is not connected at bus no. 9. The expected values of voltage unbalances at bus nos 9, 14, and 6 are 2, 1.73, and 1.23%, respectively, when the traction loads is connected at bus no. 9. It is clear that the farther distance from the asymmetric traction loads, the smaller the voltage imbalance.

The PDFs of line current unbalances in line no. 9–15, 9–14, and 4–5 are shown in Fig. 6, when the traction loads are joined and not joined at bus no. 9. Line no. 9–15 is the transmission line for powering the TS. Line no. 9–14 is near from bus no. 9 and line no. 4–5 is far from bus no. 9.

This is an open access article published by the IET under the Creative Commons Attribution License
(http://creativecommons.org/licenses/by/3.0/)

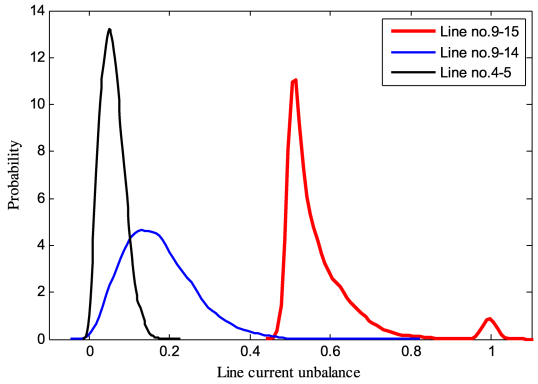


Fig. 6 *PDFs of line current unbalances in line no. 9–15, 9–14, and 4–5*

Table 1 Mean values and variances in line no. 9–15, 9–14, and 4–5

Current imbalance	Line no. 9–15	Line no. 9–14	Line no. 4–5
mean value	0.5753	0.1730	0.0584
variance	0.0115	0.0078	0.0008

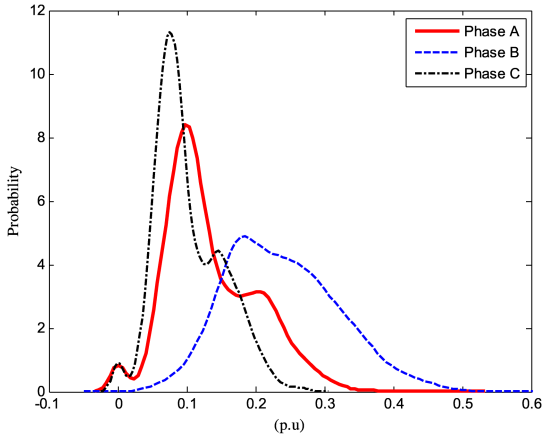


Fig. 7 *PDFs of active power in line no. 9–15*

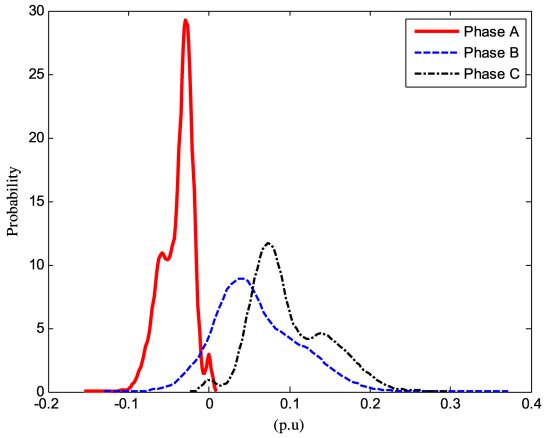


Fig. 8 *PDFs of reactive power in line no. 9–15*

Fig. 6 shows that the PDF of line current imbalance in line no. 9–15 has two peaks. The larger probability is expected 0.5753, the smaller one is expected 1. According to the theoretical analysis for V/v wiring traction transformer, the imbalance is 0.5 when both arms have the same power locomotive, and the imbalance is 1 when there is only one arm with locomotive and the other arm without locomotive. Due to the heavier transport tasks, the actual running electric locomotives exist in both supply arms. It can be seen that the actual operation of the overloaded electrified railway is better characterised by the PDF of line current imbalance in line no. 9–15.

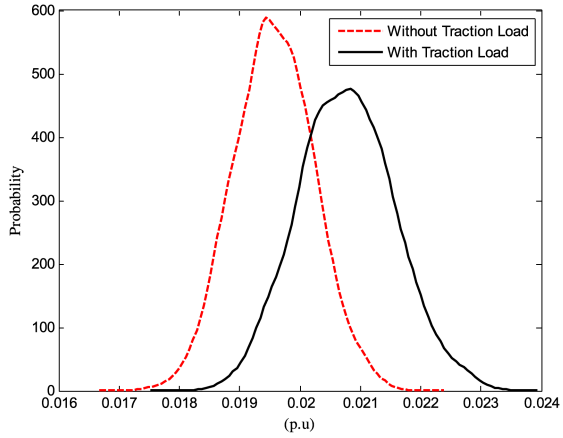


Fig. 9 *PDFs of grid loss rate*

The mean values and variances of line current imbalances in line no. 9–15, 9–14, and 4–5 are shown in Table 1.

The PDF of line current imbalance in line no. 9–14 closer to the bus no. 9 is relatively chunky, and the probability distributions are relatively scattered. The PDF of line current imbalance in line no. 4–5 farther away from the bus no. 9 is thinner and the probability distribution is more concentrated. Moreover, the farther away from the TS, the smaller the impact of asymmetry of traction loads.

5.3 Transmit power of transmission line powering to TS

The PDFs of three-phase active power and reactive power of the transmission lines powering to the TS (line no. 9–15) are shown in Figs. 7 and 8, respectively.

From the analysis of Figs. 7 and 8, it is clear that the PDFs curve of the active and reactive power of transmission lines powering to the TS are irregularly distributed. The line voltages of two arms at TS here are $\dot{U}_{AB}$ and $\dot{U}_{BC}$, respectively. The active power of Phase *B* is larger than the active power of phase *A* and phase *C*. The reactive power of phase *C*, phase *B,* and phase *A* decrease sequentially.

5.4 Impact of traction loads on grid loss

The PDF of grid loss rate is shown in Fig. 9 with and without traction loads at bus no. 9.

From Fig. 9, it is observed that the expected value of network loss without traction loads is 1.96%, and the expected value of network load with traction loads is 2.08%. Due to the asymmetric traction loads, the net loss increased by 6.12%.

6 Conclusion

The two-phase TPSS models are transformed into a three-phase equivalent model and the probabilistic model of the traction loads is established based on the number of electric locomotives and their actual operating power. The traction loads of TS in a heavy freight electrified railway is included into the modified IEEE-14 bus three-phase system. The impact of the uncertainty and asymmetry of traction loads on the high voltage grid is analysed by the probabilistic three-phase load flow. The probabilistic three-phase load flow considering traction loads is calculated using the Monte Carlo procedure. The PDFs of the phase-voltage amplitudes, voltage unbalances, line current imbalances, power of transmission line and grid loss rate are compared before and after the TPSS, which is included into the grid. With the distance TS far away, the impact of traction loads will gradually become smaller. The asymmetric traction loads connected to the grid not only cause a worsening of the unbalance in the vicinity of the grid, but also the targeted managements are required.

7 Acknowledgments

This work was supported by Youth Fund of Lanzhou Jiaotong University (2016022).

This is an open access article published by the IET under the Creative Commons Attribution License (http://creativecommons.org/licenses/by/3.0/)

8 References

[1] Li, Q.Z.: 'New generation traction power supply system and its key technologies for electrified railways', *J. Mod. Transp.*, 2015, **23**, (1), pp. 1–11

[2] Minucci, S., Pagano, M., Proto, D.: 'Model of the 2 × 25 kV high speed railway supply system taking into account the soil-air interface', *Int. J. Electr. Power Energy Syst.*, 2018, **95**, pp. 644–652

[3] He, Z.Y., Fang, L., Guo, D., *et al.*: 'Algorithm for power flow of electric traction network based on equivalent circuit of AT-fed system', *J. Southwest Jiaotong Univ.*, 2008, **43**, (1), pp. 1–7

[4] Hu, H.T., He, Z.Y., Wang, J.F., *et al.*: 'Power flow calculation of high-speed railway traction network based on train-network coupling systems', *Proc. CSEE*, 2012, **32**, (19), pp. 101–108

[5] Raygani, S.V., Tahavorgar, A., Fazel, S.S., *et al.*: 'Load flow analysis and future development study for an AC electric railway', *IET Electr. Syst. Transp.*, 2012, **2**, (3), pp. 139–147

[6] Mongkoldee, K., Kulworawanichpong, T.: 'Current-based newton-raphson power flow calculation for AT-fed railway power supply systems', *Int. J. Electr. Power Energy Syst.*, 2018, **98**, pp. 11–22

[7] Ho, T.K., Chi, Y.L., Siu, L.K., *et al.*: 'Probabilistic load flow in AC electrified railways', *IEE Proc-Electric Power Appl.*, 2005, **152**, (4), pp. 1003–1013

[8] Van Casteren, J., Groeman, F.: 'Harmonic analysis of rail transportation systems with probabilistic techniques'. Proc. Int. Conf. on Probabilistic Methods Applied to Power Systems, PMAPS, Stockholm, Sweden, June, 2006, pp. 1–6

[9] Liu, W., Li, Q.Z., Tang, B., *et al.*: 'Probabilistic load flow for urban rail traction power supply based on monte carlo simulation', *J. Southwest Jiaotong Univ.*, 2010, **45**, (4), pp. 561–567

[10] Caramia, P., Carpinelli, G., Varilone, P., *et al.*: 'Probabilistic three-phase load flow', *Int. J. Electr. Power Energy Syst.*, 1999, **21**, (1), pp. 55–69

[11] Gupta, N., Daratha, N.: 'Probabilistic three-phase load flow for unbalanced electrical systems with wind farms', *Int. J. Electr. Power Energy Syst.*, 2017, **87**, pp. 154–165

[12] Li, Q.Z.: '*Traction substation power supply analysis and comprehensive compensation technology*' (China Railway Press, Peking, 2006)

[13] Satoshi, S., Jumpei, B., Katsuhiko, S., *et al.*: 'Effective application of superconducting magnetic energy storage (SMES) to load levelling for high speed transportation system', *IEEE Trans. Appl. Supercond.*, 2004, **14**, (2), pp. 713–716

[14] Yang, S.B., Wu, M.L.: 'Power load modelling and parameter identification based on improved ant colony algorithm for passenger lines', *Proc. CSEE*, 2015, **35**, (7), pp. 1578–1585

[15] 'Power systems test case archive'. https://www2.ee.washington.edu/research/pstca/, accessed 18 January 2018

This is an open access article published by the IET under the Creative Commons Attribution License (http://creativecommons.org/licenses/by/3.0/)